Bitlis Eren Üniversitesi Fen Bilimleri Dergisi
BİTLİS EREN UNIVERSITY JOURNAL OF SCIENCE
ISSN: 2147-3129/e-ISSN: 2147-3188
VOLUME: 13 NO: 4 PAGE: 999-1012 YEAR: 2024
DOI: 10.17798/bitlisfen.1490837

Development of a Functionalized SiO_2 Supported Ni Nanoparticles Based Non-Enzymatic Amperometric Dopamine Sensor

Yunus Emre YILDIRIM[1], Muhammet GÜLER[1*]

[1]*Van Yüzüncü Yıl University, Faculty of Science, Department of Chemistry, Van, Turkiye (ORCID: 0009-0004-5813-8640) (ORCID: 0000-0002-1040-8988)*

Keywords: Sensor, Functionalized SiO_2, Ni nanoparticles, Dopamine

Abstract

In the present work, a novel electrochemical dopamine (DA) sensor depending on Nickel (Ni) nanoparticles decorated (3-aminopropyl)triethoxysilane (APTES) modifed silica (SiO_2) was fabricated. Hence, Ni@SiO_2-APTES was synthesized by the conventional wet-impregnation method. The structure of the compozite was evaluated using Fourier transform infrared spectroscopy (FTIR), Scanning electron microscopy-energy dispersive X-ray (SEM-EDX), and X-ray diffraction (XRD). The synthesized Ni@SiO_2-APTES was loaded on glassy carbon working electrode (GCE). Also, Nafion (Nf) was drop-casted on Ni@SiO_2-APTES/GCE to stabilize the electrode. The fabricated Nf/Ni@SiO_2-APTES/GCE working electrode was electrochemicaly evaluated using cyclic voltammetry (CV), electrochemical impedance spectroscopy (EIS) and amperometry. CV and EIS results indicated that Ni nanoparticles increased both the conductivity and sensitivity of the working electrode. The linear detection range for DA was found to be 0.2 – 252 µM with limit of detection (LOD) was 0.07 µM depending on S/N of 3. The sensitivity was found to be 578.26 µA mM^{-1} cm^{-2} depending on the active surface area of the modified working electrode. The sensor exhibited excellent selectivity in the electrolyte solution including ascorbic acid, glucose, fructose, sucrose, mannose, uric acid, and phenylalanine. The sensor had satisfactory repeatability and reproduciblity. It was observed that the sensor showed an electrocatalytic response of 95.33% after 28 days. According to this result, it was concluded that the sensor was extremely stable within the studied time period. The applicability of Nf/Ni@SiO_2-APTES/GCE was tested using dopamine HCl injection (200 mg/5 mL).

1. Introduction

Enzyme-based electrochemical biosensors appear to be ideal materials for the determination of target analytes due to their high selectivity. However, in the in vitro environment, factors such as temperature, pH and binding of the biomolecule to the surface of the electrode can shorten the working life of the biosensor. Further studies are needed to increase the stability of such biosensors, and new fabrication techniques should be developed for easier preparation of biosensors. Contrary to enzyme-based electrochemical sensors, non-enzymatic sensors have high stability, satisfactory selectivity and are relatively easy to prepare. Non-enzymatic electrochemical sensors have been shown to remain electrochemically active in undiluted blood for more than 30 days, which is not possible with enzyme-based sensors. However, there are fundamental difficulties such as the use of alkaline working environments especially for the determination of analytes such as glucose and the expensiveness of the materials used [1].

Dopamine, known as [4-(2-aminoethyl) benzene-1,2-diol], is a significant catecholamine substance widely secreted in the cerebrospinal fluid of mammals and the main member of the neurotransmitter's family. Dopamine has a significant impact in cardiovascular functions, hormonal, renal and central nervous systems. High or low dopamine levels can cause diseases such as tourette syndrome [2], schizophrenia [3], hyperactivity, attention deficit [4] and tumor formation [5]. It has been concluded that insufficient dopamine levels in the brain can lead

*Corresponding author: mguler@yyu.edu.tr
Received: 27.05.2024, Accepted: 11.12.2024

to involuntary muscle activity in Parkinson's disease [6], while excessive amounts can lead to Huntington's disease [7]. Given the critical function of this substance in the metabolism, a lot of efforts have been made to identify this biogenic amine. Dopamine has been determined in biological fluids and pharmaceutical drugs using a variety of methods, including electrochemical, UV-visible spectrophotometry, high-performance liquid chromatography (HPLC), liquid chromatography/mass spectrometry (LC/MS), fluorometry, and capillary zone electrophoresis [8], [9]. Electrochemical sensors/biosensors are one of these techniques with numerous benefits. For example, they are cheap, easy to prepare, not complex systems, and exhibit rapid responses [10]. Electrochemical biosensors are not complicated to install and costly to fabricate compared to other measurement techniques such as HPLC and LC/MS. The reason for this can be considered as the production of relatively low-cost microelectronic circuits and the fabrication of interfaces that can easily respond to the target analyte. In addition, other advantages of electrochemical sensors include their robustness, easy miniaturization, excellent response to even small analyte concentrations, and the ability to provide this response within seconds [11], [12].

For the design of electrochemical sensors, nanocomposites have been prepared by deposition of nanoparticles such as metal and metal oxide on supports including carbon nanotube [13], graphene oxide, reduced graphene oxide [14], and SiO_2 [15].

By modifying the working electrodes with these nanocomposites, the determination of electrochemically active substances like hydrogen peroxide, dopamine, ascorbic acid, folic acid and paracetamol was achieved [16], [17]. However, the performance factors such as LOD, linear determination range, especially repeatability, reproducibility, and storage stability of these sensors need to be improved.

Silica (SiO_2), which has a large surface area, was used as a support material, allowing metal and metal oxide nanoparticles to be dispersed uniformly on the surface [15], [18]. Surface-modified silica can enhance the electrocatalytic performance of metal or metal oxide nanoparticles. For example, in a study performed by Bayram and Guler, an electrochemical hydrogen peroxide sensor depending on Au nanoparticles deposited on SiO_2-APTES was designed. The SiO_2-APTES support provided an excellent surface for the deposition of Au nanoparticles on the surface. Because both low diameter of Au nanoparticles (mean particle size of 3.05 ± 0.14 nm) were deposited on the surface and it was determined that the nanoparticles were homogeneously distributed on the support. A very high sensitivity for hydrogen peroxide (2514.6 μA mM^{-1} cm^{-2} between 0.014 and 0.18 mM and 894.2 μA mM^{-1} cm^{-2} between 0.18 and 7.15 mM) was achieved depending on the conductivity and size of the Au nanoparticles deposited on the support [17].

The purpose of the present work is to prepare an electrochemical DA sensor using Ni@SiO_2-APTES modified glassy carbon electrode (GCE). The specific aims are (i) to synthesize Ni@SiO_2-APTES, (ii) to modify GCE using Ni@SiO_2-APTES and, (iii) to detect performance factors such as linear range, LOD, and selectivity for DA using amperometry and cyclic voltammetry.

2. Material and Method

Silica (SiO_2, 240-400 mesh), ethanol, anhydrous ethanol, and sodium borohydride ($NaBH_4$) were purchased from Merck Company. (3-Aminopropyl)triethoxysilane (APTES), dopamine hydrochloride (DA), nickel (II) nitrate hexahydrate $Ni(NO_3)_2.6H_2O$, nafion (Nf) solution (5% in a mixture of aliphatic alcohol and water), potassium chloride (KCl) , glucose (Glu), sucrose (Suc), fructose (Fruc), Monnose (Man), ascorbic acid (AA), uric acid (UA), toluene, boric acid (H_3BO_3), acetic acid (CH_3COOH), phosphoric acid (H_3PO_4), acetone, sodium hydroxide (NaOH), hydrochloric acid (HCl) were acquired from Sigma-Aldiric Company and All other chemicals used were purchared from Merck Company. In the electrochemical studies, glassy carbon electrode (GCE of 3 mm diameter) was used as the working electrode, Ag/AgCl (3 M KCl) as the reference electrode, and platinum wire as the counter electrode was purchased from BASİ company. For the electrochemical studies, Autolab brand PGSTAT128N model potentiostat/galvanostat device containing the FRA 32M module was used.

The characterization of the samples was monitored by Field emission scanning electron microscope (FE-SEM; Zeiss sigma 300) and Fourier transform infrared spectroscopy (FTIR) at Van Yüzüncü Yıl University Science Application and Research Center. X-ray diffraction (XRD) was performed at Selçuk University Advanced Technology Research and Application Center.

2.1. Synthesis of SiO_2-APTES and Ni@SiO_2-APTES composites

Before attached APTES to SiO_2, SiO_2 was dried in an oven (JP Selecta S. A., Spain**)** at 100 °C. 2 g of dried SiO_2 was included in 30 mL of pure toluene and

stirred for a while. Then, 5.4 mL APTES was included in the mixture and it was stirred for 24 hours. After the reaction was completed, the mixture was filtered and cleaned down using toluene (5x20 mL). The washed SiO_2-APTES was dried in the oven at 100 °C for 1 hour [19].

Ni@SiO_2-APTES was synthesized by the conventional wet-impregnation method. For this, 0.1 g support was put in 5 mL ultra-pure water and mixed in an ultrasonic cleaner for 10 min. Then, 26.06 mg $Ni(NO_3)_2x6H_2O$ (5% Ni) was put into the above mixture and stirred for 3 hours using a magnetic stirrer. 50.84 mg $NaBH_4$ (1.344mmol) was included in the mixture and it was stirred until the reduction was completed. The resulting Ni@SiO_2-APTES nano composite was filtrated and then washed with ethanol (3x20 mL) and water (3x20 mL), respectively, and dried in the oven at 100 °C. To achieve the best sensor response, Ni@SiO_2-APTES was obtained by using different ratio of Ni salt (2, 5, 10, 15 and 20%) [20]. The fabrication of Nf/Ni@SiO2-APTES/GCE working electrode and its electrochemical response to DA is given step by step in Scheme 1.

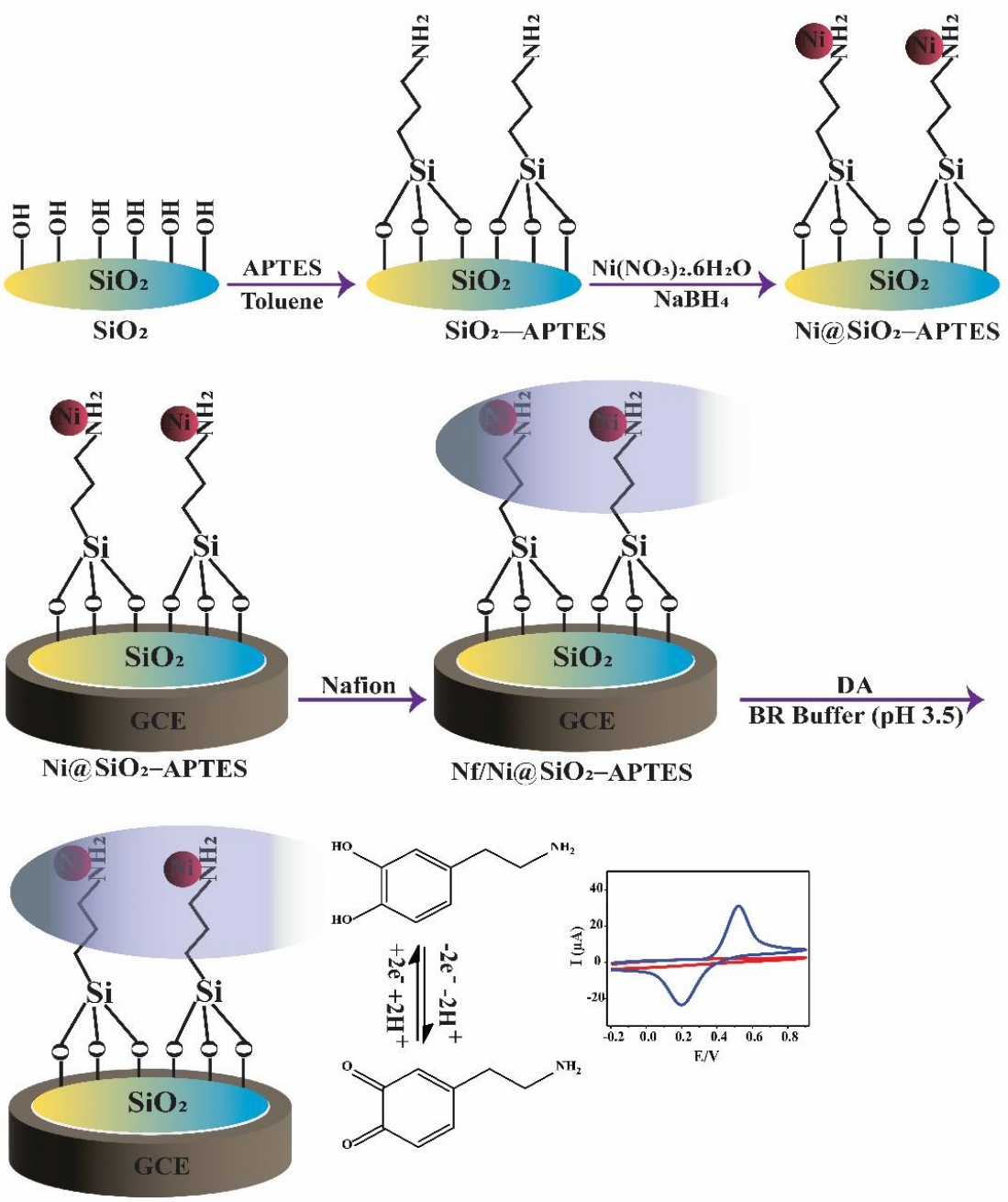

Scheme 1. Step by step fabrication of Nf/Ni@SiO_2-APTES/GCE working electrode and its electrochemical response to DA.

2.2. Fabrication of working electrodes

In the study, the working electrode, the GCE, was polished using Al_2O_3 slurry before being modified. Afterwards, it was cleaned using nitric acid/pure water prepared in the ratio of (1:1) and acetone in an ultrasonic bath. 5 µL of 2 mg/mL Ni@SiO_2-APTES mixture was dropped onto the GCE. The fabricated electrode was dried in the laboratory temperature. Then, 3 µL of 0.3% Nf solution was loaded on the electrode and the electrode was left to dry [17]. The obtained Nf/Ni@SiO_2-APTES/GCE was used for further electrochemical studies.

3. Results and Discussion

The structural properties of the obtained SiO_2-APTES were evaluated using FTIR. Figure 1 shows the FTIR spectrum of SiO_2 and SiO_2-APTES. Figure 1a shows the general FTIR peaks of the SiO_2 compound. The peaks at 794, 972 and 1056 cm^{-1} show the Si-O symmetric bending vibration peak, Si-O-(H-H_2O) bending vibration peak and Si-O-Si asymmetric vibration peak, respectively. Figure 1b shows the FTIR spectrum of SiO_2-APTES composite. As seen in the figure, the peaks occurring at 696, 790, 1062, 1392, 1537, 2902 and 2978 cm^{-1} show the characteristic vibration peak of the Si-CH_2 group, symmetric bending vibration peak of Si-O, asymmetric vibration peak of Si-O-Si, the stretching vibration peak of C-N, the bending vibration peak of the N-H group, and the stretching vibration peak of the C-H groups, respectively. Additionally, it can be seen that the peak at 972 cm^{-1} disappears after APTES is attached to the SiO_2. This is due to the reaction that occurs between the ethoxy groups in the APTES and Si-OH groups [21], [22].

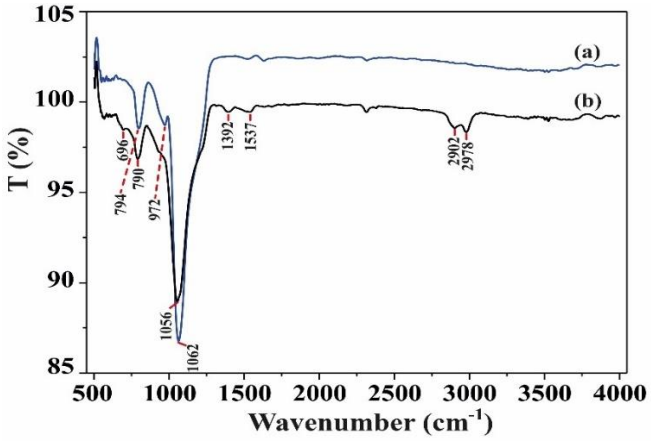

Figure 1. FTIR spectrum of (a) SiO_2 and (b)SiO_2-APTES.

The crystal structure of SiO_2-APTES and Ni@SiO_2-APTES composites was investigated using XRD (Figure 2). Figure 2a and Figure 2b show the XRD spectra of SiO_2-APTES and Ni@SiO_2-APTES structures, respectively. As seen in Figure 2b, even though 5% nickel salt was used, a weak peak was formed at about 2θ = 45°. In this study, $NaBH_4$, a good reducing agent, was used to reduce Ni nanoparticles on SiO_2-APTES support. This shows that the Ni-B amorphous structure forms by sodium borohydride with Ni at room temperature [23], [24].

SEM-EDX was used to investigate the surface properties of SiO_2-APTES and Ni@SiO_2-APTES composites. Figures 3A and 3B show SEM pictures of the synthesized SiO_2-APTES support obtained at 30 µm and 200 nm. Figures 3C and 3D display SEM images of the Ni@SiO_2-APTES obtained at 400 and 200 nm. Figure 4A exhibits the SEM image of the Ni@SiO_2-APTES composite, and the energy dispersion X-ray (EDX) spectra of the selected region is seen in Figure 4B. The weight of the Ni obtained in the spectrum is 6.78%, and this value is close to the 5% value, which is the weight percentage of Ni in the Ni salt used to synthesize the Ni@SiO_2-APTES composite in the experimental section. The presence of carbon and nitrogen in the EDX graph shows that the APTES compound was bound on SiO_2 support. Figures 4C/D/E/F show the elemental mapping images of the composite.

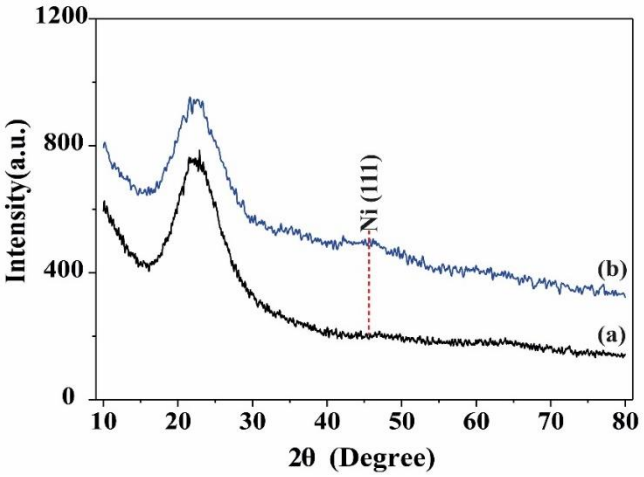

Figure 2. XRD graph of (a) SiO_2-APTES and (b) Ni@SiO_2-APTES.

CV and EIS methods were performed to evaluate the electrocatalytic properties of the working electrodes and evaluate their electrocatalytic responses to DA. For this purpose, firstly, CVs at GCE, Nf/SiO_2-APTES/GCE and Nf/Ni@SiO_2-APTES/GCE working electrodes were obtained in BR buffer (pH 3.5) in the absence and presence

of DA at the scan rate of 50 mV/s and the potential range of -0.2 to 0.8 V (Figure 5A and 5B). As can be seen in Table 1, it was displayed that the anodic peak current of the Nf/Ni@SiO_2-APTES/GCE was approximately 1.5 times the anodic peak current of the Nf/SiO_2-APTES/GCE. The rate of oxidation and reduction peak currents of the Nf/Ni@SiO_2-APTES/GCE was calculated as I_{pa}/I_{pc} = 1.076. This shows that a quasi-reversible electrode process occurs on the Nf/Ni@SiO_2-APTES/GCE electrode. In additon, as illustrated in Figure 6C, an increase in scan rate results in an increase in the redox peak potential difference (ΔEp). The increment in the peak potential difference depending on the scan rate indicates a quasi-reversible reaction process [9].

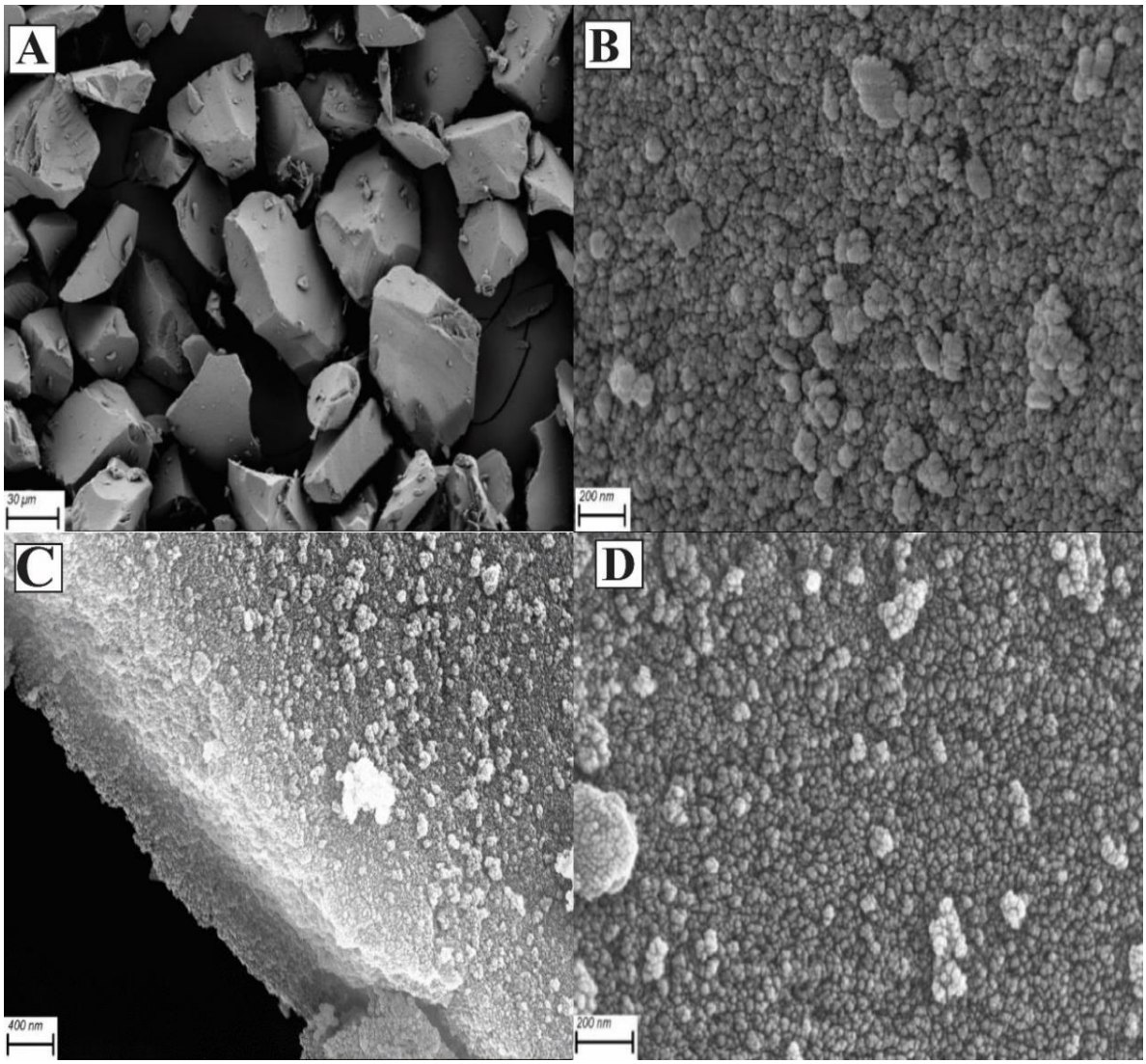

Figure 3. SEM images of (A, B) SiO_2-APTES and (C, D) Ni@SiO_2-APTES.

Table 1. Some electrochemical response data of working electrodes to DA.

Electrode	$i_{pa}/\mu A$	$i_{pc}/\mu A$	E_{pa}/V	E_{pc}/V	i_{pa}/i_{pc}	ΔE_p
GCE	2.53	-2.26	0.564	0.235	1.119	0.329
SiO_2-APTES	6.74	-6.59	0.474	0.247	1.023	0.227
Ni@SiO_2APTES	9.69	-9.01	0.466	0.252	1.076	0.214

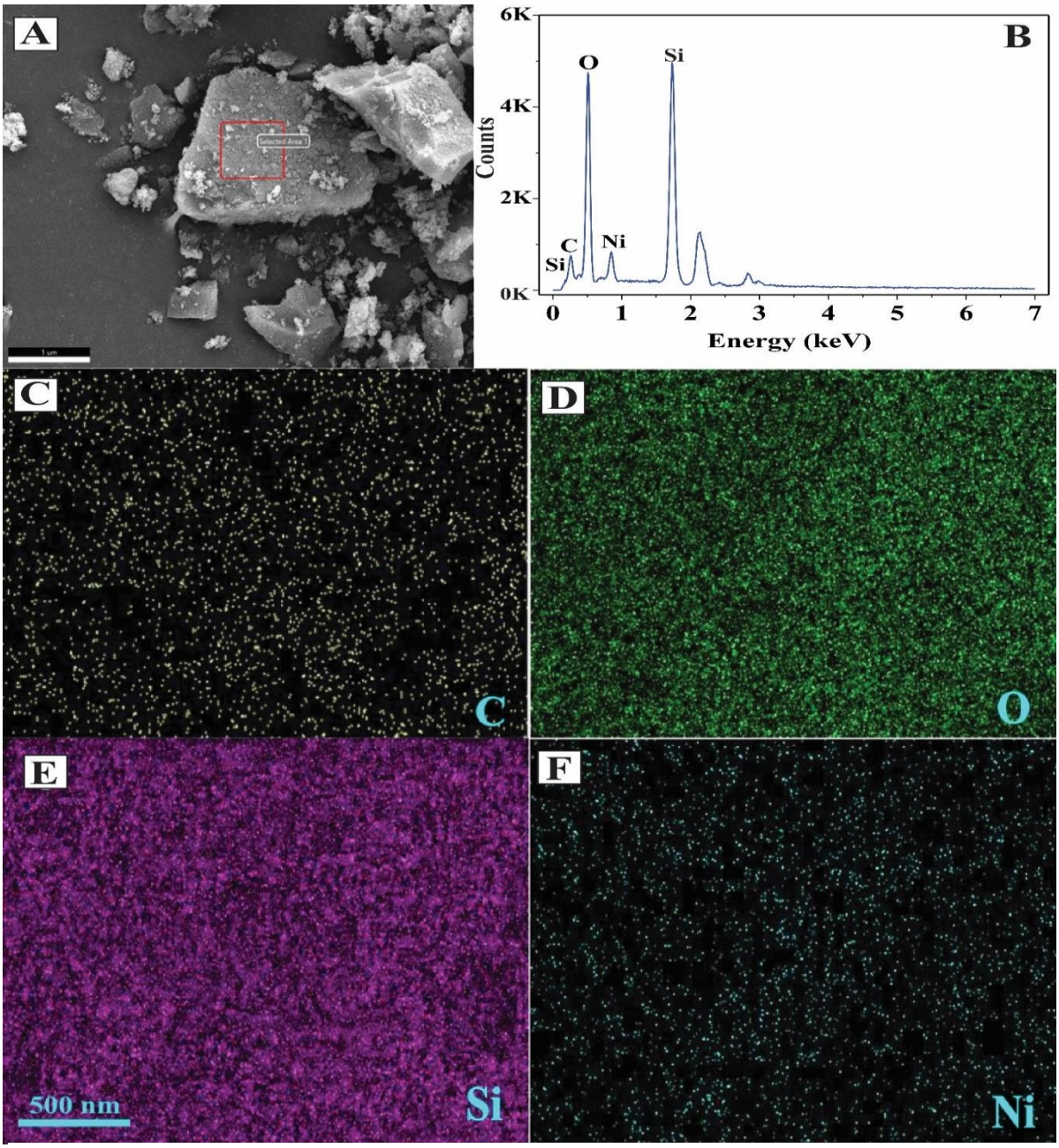

Figure 4. SEM image of (A) Ni@SiO_2-APTES, EDX of Ni@SiO_2-APTES, elemental mapping pictures of carbon (C), oxygen (D), silisium (E), and nickel (F).

Figure 5C shows the typical EIS Nyquist plot for GCE, Nf/SiO_2-APTES/GCE, and Nf/Ni@SiO_2-APTES/GCE electrodes. Nyquist curves were obtained in a solution containing 5 mM $[Fe(CN)_6]^{3-}$/$[Fe(CN)_6]^{4-}$ and 0.1M KCl. The used frequency interval and potential value were 0.1 Hz-100 kHz and 0.2 V, respectively. As shown in the figure, the Nyquist plot contains a semicircular region at high frequency and a linear domain at low frequency. In the resulting graph, the charge transfer resistance is equal to the semicircle's diameter (R_{ct}) [25]. By using these plots, R_{ct} data were calculated as 178 Ω for GCE, 25.5 kΩ for Nf/SiO_2-APTES/GCE and 7.55 kΩ for Nf/Ni@SiO_2-APTES/GCE. According to these values, it is seen that the charge transfer resistance of the Nf/Ni@SiO_2-APTES/GCE decreased after Ni nanoparticles was deposited on the support.

Ni@SiO_2-APTES nanocomposites containing different amounts of Ni (2, 5, 10, 15, and 20%) were synthesized to determine the Ni percentage which exhibits the best electrochemical response to DA. Nf/Ni@SiO_2-APTES/GCE were prepared using these nanocomposites. Then, CVs were obtained in BR (pH 3.5) buffer containing 0.2 mM DA (Figure 5D). The anodic peak current values

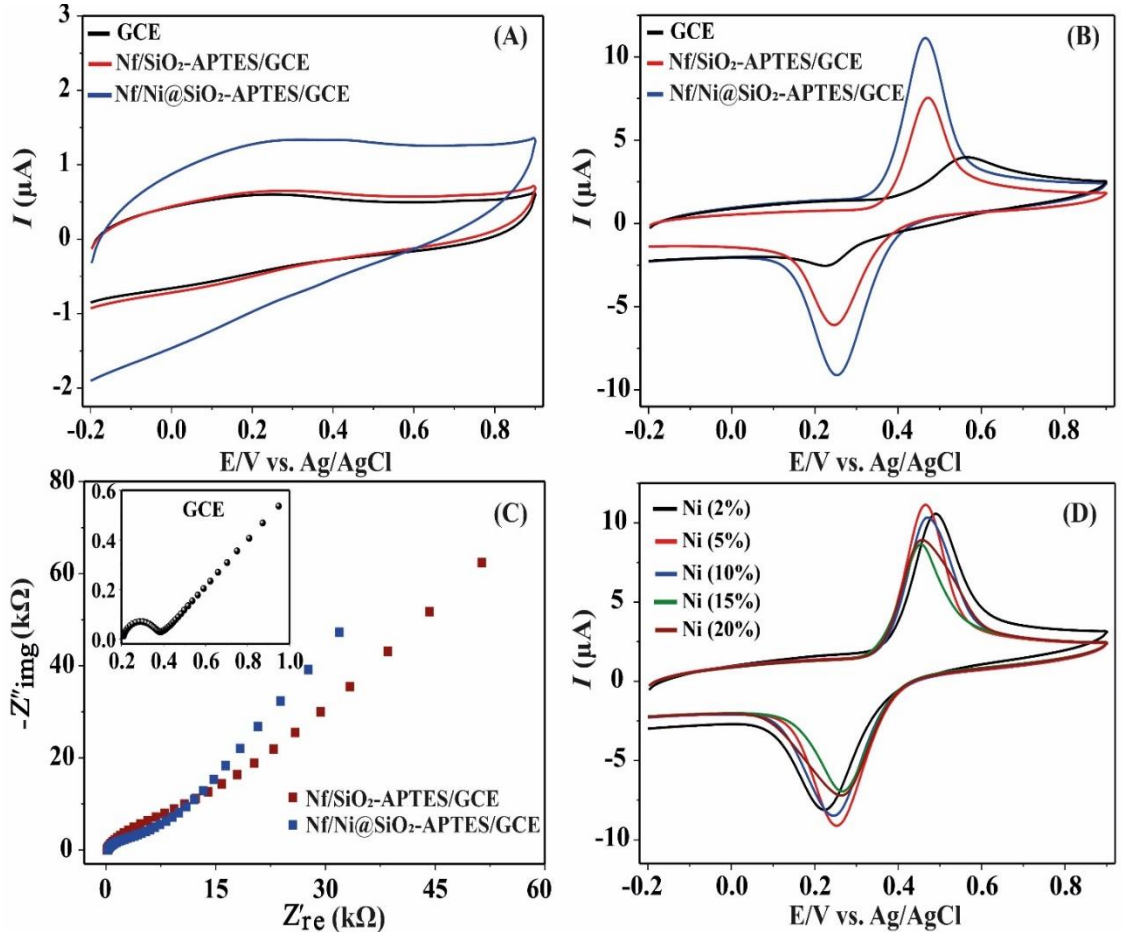

Figure 5. (A) CVs of GCE, Nf/SiO_2-APTES/GCE, and Nf/Ni@SiO_2-APTES in BR buffer (pH 3.5) in the absence of DA. (B) CVs of GCE, Nf/SiO_2-APTES/GCE, and Nf/Ni@SiO_2-APTES in BR buffer (pH 3.5) in the presence of DA at the scan rate of 50 mV/s. (C) Nyquist graph of GCE, Nf/SiO_2-APTES/GCE, and Nf/Ni@SiO_2-APTES obtained in 5 mM $[Fe(CN)_6]^{3-}$/$[Fe(CN)_6]^{4-}$ and 0.1M KCl. (D) Effect of Ni ratio on the redox reaction of DA.

of DA of these voltammograms were compared. The oxidation peak currents of the sensors were 8.89 µA for 2% Ni, 9.77 µA for 5% Ni, 8.98 µA for 10% Ni, 7.29 µA for 15% Ni and 7.56 µA for 20% Ni. According to these results, Nf/Ni@SiO_2-APTES (5% Ni) exhibited the highest oxidation peak current and electrochemical measurements were performed using this ratio.

In our study, BR buffer, which has a wide buffering range (2-12), was used to investigate the influence of the pH of the electrolyte on the redox behavior of DA. Figure 6A shows CVs obtained in BR buffer with different pH values (3-8). Current-pH and potential-pH graphs were drawn by means of these voltammograms (Figure 6B). The linear equation obtained for the potential-pH graph was E_{pa} = - 0.0462pH + 0.605 (R^2 = 0.9875). The equation's slope was computed to be 46.2 mV/pH, which is comparable to the Nernts equation's slope of 59 mV/pH. In some previous studies, it is thought that two proton ($2H^+$) and two electron ($2e^-$) transfers occur in the anodic reaction of DA to form dopamine-o-quinone [26], [27], [28]. As can be seen from the graph, the anodic peak current of DA increases as the pH of the electrolyte decreases. BR buffer with pH 3.5 was used in electrochemical studies by taking into account the electrochemical performance of the working electrode. In addition, the oxidation peak potential shifted to the negative direction as the pH value incremented. This means that protons participate in the electrochemical reaction [29].

The following Laviron equations were used to determine the number of electrons getting in on the electrochemical reaction and the charge transfer coefficient (1 eq. and 2 eq.) [30].

$$E_{pc} = E^{\circ} - \frac{RT}{\alpha nF} lnv \quad (1)$$

$$E_{pa} = E^{\circ} + \frac{RT}{(1-\alpha)nF} lnv \quad (2)$$

In the above equations, *n* is the number of electrons taking part in the reaction, *α* is the charge transfer coefficient, *υ* is the scan rate, *R* is the gas constant (8.314 j/mol K), *T* is the temperature in kelvin, and F is the Faraday constant (96485 C/mol). For this purpose, CVs were achieved at various scan rates (0.02-0.4 V/s) in BR (pH 3.5) buffer containing 0.2 mM DA (Figure 6C). The relationship between the reduction and oxidation peak potentials and *lnυ* is seen in Figure 6D. The linear equations were found to be E_{pa} = 0.0298*lnυ* + 0.5335 (R^2 = 0.9978) and E_{pa} = -0.0333*lnυ* + 0.1356 (R^2 = 0.9983). The slopes of these equations are equal to the slopes in the Laviron equations (1 eq. and 2 eq.), and n and α were computed to be 1.63 ~ 2 and 0.47, respectively. These values were found to be consistent with previous studies. For example, in a study by Gong and his colleagues, an electrochemical sensor was prepared using poly-tryptophan-functionalized graphene. In the study, α and n values were calculated as 0.67 and 1.65, respectively [31]. The electrochemical oxidation and reduction reaction of DA can be written as given in Scheme 2.

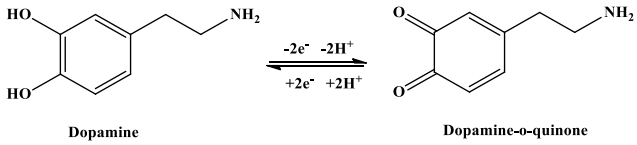

Scheme 2. The electrochemical oxidation and reduction reaction of DA

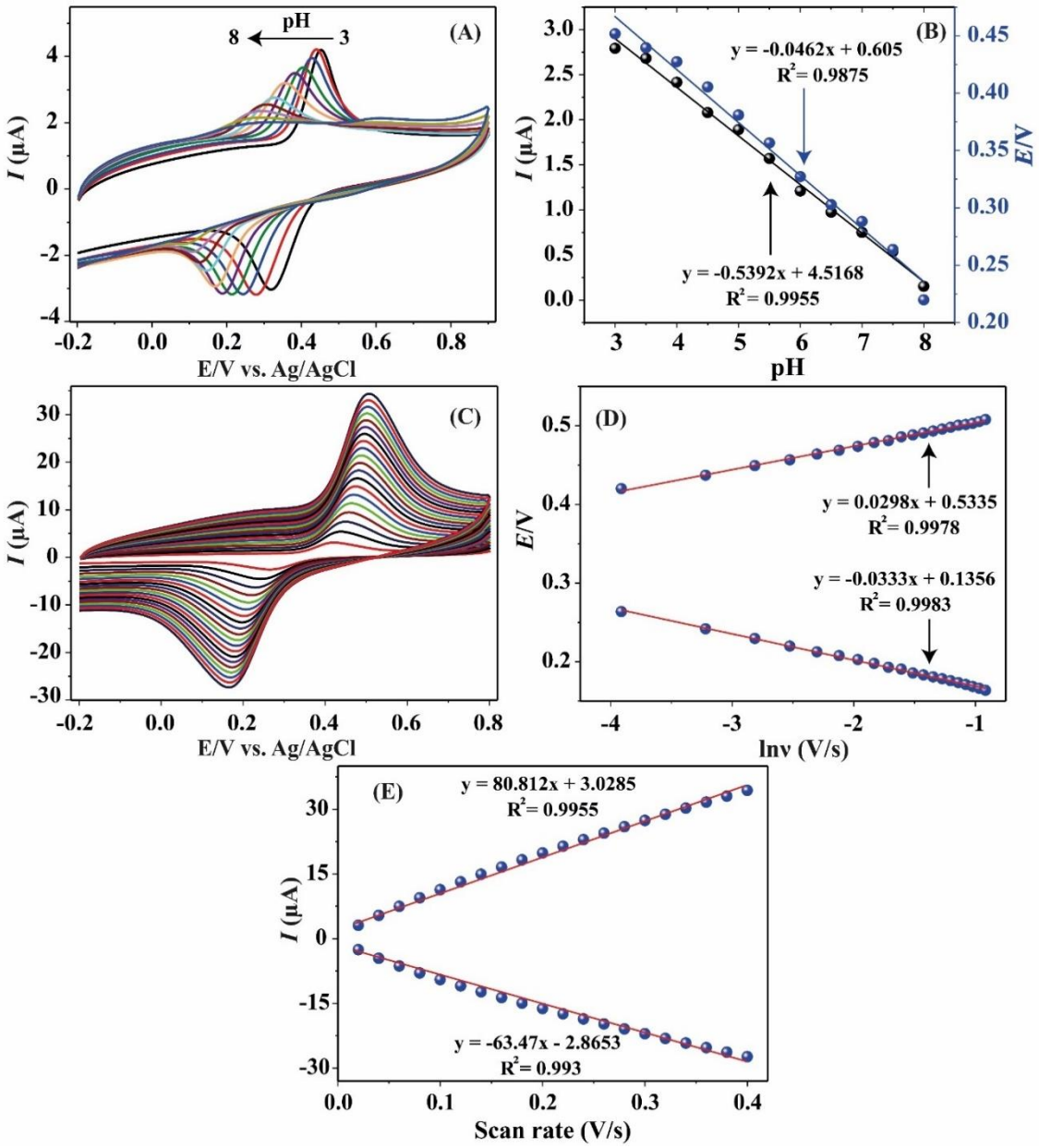

Figure 6. (A) CVs obtained by Nf/Ni@SiO_2-APTES in BR buffer with various pH (3, 4, 5, 6, 7, and 8) PBS solution. (B) *I* (μA) *vs.* pH graph. (C) CVs obtained at various scan rates (from 0.02 to 0.4 V/s). (D) *E* (V) *vs.* lnv graph. (E) *I* (μA) vs. scan rate (V/s) graph.

In order to detect the type of the reaction process of DA on the working electrode, the oxidation and reduction peak currents versus scan rate graph was obtained using CVs obtained at different scan rates (Figure 6E). According to the graph, it was concluded that both oxidation and reduction peak currents were linear against the scan rate. These results show that the electrode reaction of DA is an adsorption-controlled process [32].

In our study, DA was determined using both cyclic voltammetry and amperometric methods. For this purpose, the voltammograms were obtained by adding different concentrations of DA to BR (pH 3.5) buffer solution (Figure 7A). Using the oxidation peak current values of these voltammograms, the graph of concentration of DA versus peak current value was obtained. As seen in Figure 7B, two linear determination ranges were obtained. The first linear equation is I (μA) = 48.991[DA] (mM) + 2.2531 (R^2 = 0.9916) and the second linear equation is I (μA) = 27.681[DA] (mM) + 10.684 (R^2 = 0.9952). The sensitivities were computed to be 2130.04 μA mM^{-1} cm^{-2} and 1203.52 μA mM^{-1} cm^{-2}, respectively. The LOD was detected to be 0.36 μM depending on 3xSD/Slope. The linear detection range, sensitivity and limit of detection (LOD) values of the sensor for DA were determined using amperometry. Figure 7C shows the current-time graph obtained at 0.44 V potential using the amperometric method. Figure 7D exhibits the current-DA concentration graph. The linear equation of the graph was determined as I (μA) = 0.0133[DA] (μM) + 0.0596 (R^2 = 0.9974). The linear detection range for DA was $2x10^{-7}$ – $2.52x10^{-4}$ M. The sensitivity of the sensor was calculated to be 578.26 μA mM^{-1} cm^{-2} depending on the active surface area of the working electrode. The active surface area of each working electrode was achieved using The Randles-Sevcik equation [33]. The active surface area was detected to be 0.092 cm^2 for GCE, 0.004 cm^2 for Nf/SiO_2-APTES/GCE, and 0.023 cm^2 for Nf/Ni@SiO_2-APTES. Due to the low conductivity of the SiO_2-APTES, it showed a lower active surface area than the bare electrode. However, after Ni was deposited on the surface of the support, the active surface area of the working electrode increased by 5.75 times. The LOD value of the sensor was 0.07 μM depending on the signal-to-noise ratio of 3. Due to both the working environment and the high sensitivity of the device used, high noise was obtained at the high analyte concentrations of DA when using amperometric measurement. For this purpose, one linear determination range was determined by the amperometric method when compared with the CV method. In addition, CV is mostly used to evaluate the reduction/oxidation process of the target analyte.

To date many studies have been carried out to determine electrochemically DA. For example, in one study performed by Gong et al., the glassy carbon electrode was modified using polytryptophan-functionalized graphene. DA was determined in the range of 0.2-100 μM using the differential pulse voltammetric method and the LOD value of the sensor was found to be 0.06 μM. DA was successfully determined in dopamine injections using the sensor [34]. In another study, flower-like gold nanoparticles were deposited on the gold electrode using the potentiostatic electrochemical deposition method. The resulting nanostructures had large surface areas, and ascorbic acid (AA) and DA were determined selectively and sensitively. DA was determined in the linear range of 1-150 μM and the LOD value of the sensor was found to be 0.2 μM [35]. In one study, the working electrode was modified using platinum–silver graphene (Pt–Ag/Gr) nanocomposite for the determination of DA. CV and differential pulse voltammetry (DPV) were used in electrochemical studies for DA determination. CV results indicated that Pt–Ag/Gr/GCE increased the electrocatalytic response to DA electro-oxidation because of the synergistic influence between platinum-silver nanoparticles and graphene. The sensor displayed a linear detection range of 0.1-60 μM with a detection limit of 0.012 μM for DA using DPV method [36]. In a study reported by Li et al., Ag nanoparticles deposited on CuO porous nanobelts (Ag/CuO PNPs) were prepared for DA detection. DA electrochemical sensor was developed using Ag/CuO. The linear detection range was 0.04-10 μM with LOD of 7 nM [37]. In a study by Xue and colleagues, DA was determined amperometrically using gold nanoparticles (AuNPs) doped molecularly imprinted polymers (MIPs). The electrode exhibited a linear range from 0.02 to 0.54 μM and a LOD of 7.8 nM [38]. In our study the constructed Nf/Ni@SiO_2-APTES/GCE electrochemical sensor displayed a linear range between 0.2 and 252 μM with LOD of 0.07 μM and sensitivity of 578.26 μA mM^{-1} cm^{-2}. Considering these values obtained, the sensor showed a satisfactory linear determination range and detection limit.

So as to evaluate the selectivity of the Nf/Ni@SiO_2-APTES/GCE electrode, ascorbic acid (AA), uric acid (UA), phenylalanine (Phe), glucose (Glu), fructose (Fruc), mannose (Man) and sucrose (Suc) were used. Figure 8A shows the current-time graph obtained using various concentrations of DA (0.4, 1.0, 4.0 and 10.0 μM) and 25 μM AA, UA, Phe, Glu, Fruc, Man and Suc. As seen from the figure, the sensor did not show a remarkable electrocatalytic response to these compounds. This shows that the

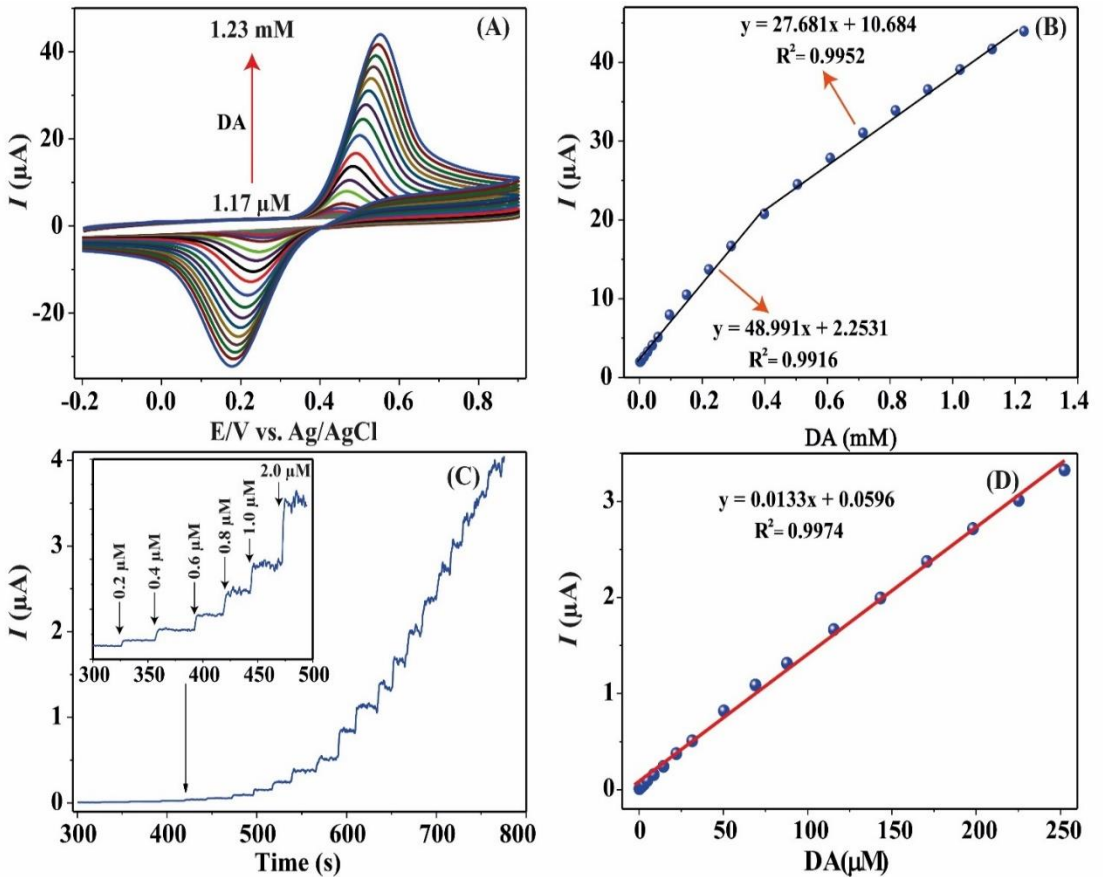

Figure 7. (A) CVs obtained by Nf/Ni@SiO_2-APTES/GCE in BR buffer (pH 3.5) containing various amount of DA at the scan speed of 50 mV/s. (B) I (µA) vs. DA concentration graph. (C) Amperometric response obtained using Nf/Ni@SiO_2-APTES/GCE on successive addition of DA to BR buffer (pH 3.5) at the performed potential of 0.44 V. (D) I (µA) vs. DA concentration graph.

sensor has excellent selectivity toward DA against these substances used.

To investigate the repeatability, 0.4, 1.0, 4.0 and 10.0 µM DA were measured using the same Nf/Ni@SiO_2-APTES/GCE working electrode. Figure 8B shows the current-DA concentration graph. The relative standard deviation (RSD) values were 5.46% for 0.4 µM DA, 3.22% for 1.0 µM DA, 2.7% for 4.0 µM DA, and for 2.6% for 10.0 µM DA. These findings indicated that the sensor has satisfactory repeatability.

To evaluate the reproducibility of the sensor, five Nf/Ni@SiO_2-APTES/GCE sensors were prepared under the same conditions. Then, electrochemical response of these electrodes to 0.4, 1.0, 4.0 and 10.0 µM DA were obtained. Figure 8C exhibits current-DA concentration graph. The RSD values were calculated as 3.9% for 0.4 µM DA, 1.87% for 1.0 µM DA, 0.6% for 4.0 µM DA, and 3.08% for 10.0 µM DA. According to these results, the sensor exhibited satisfactory reproducibility.

In our study, dopamine hydrochloride injection was used for real sample analysis. For this purpose, injection containing 200 mg/5mL dopamine hydrochloride were purchased from a local pharmacy and 0.1 and 1.0 mM DA solutions were prepared. Different concentrations of DA were put into the cell containing BR (pH 3.5). After that, the current-time graph was obtained. The mean value, standard deviation (SD) and RSD values was calculated for DA concentrations. Table 2 shows the RSD and recovery values with the DA concentrations added and found in the electrochemical cell, demonstrating that DA can be determined in dopamine injection using Nf/Ni@SiO_2-APTES/GCE sensor.

The storage stability of Nf/Ni@SiO_2-APTES/GCE was tested for 28 days. The sensor showed an electrocatalytic response of 95.33% after 28 days. It was concluded that the sensor was extremely stable within the studied time period.

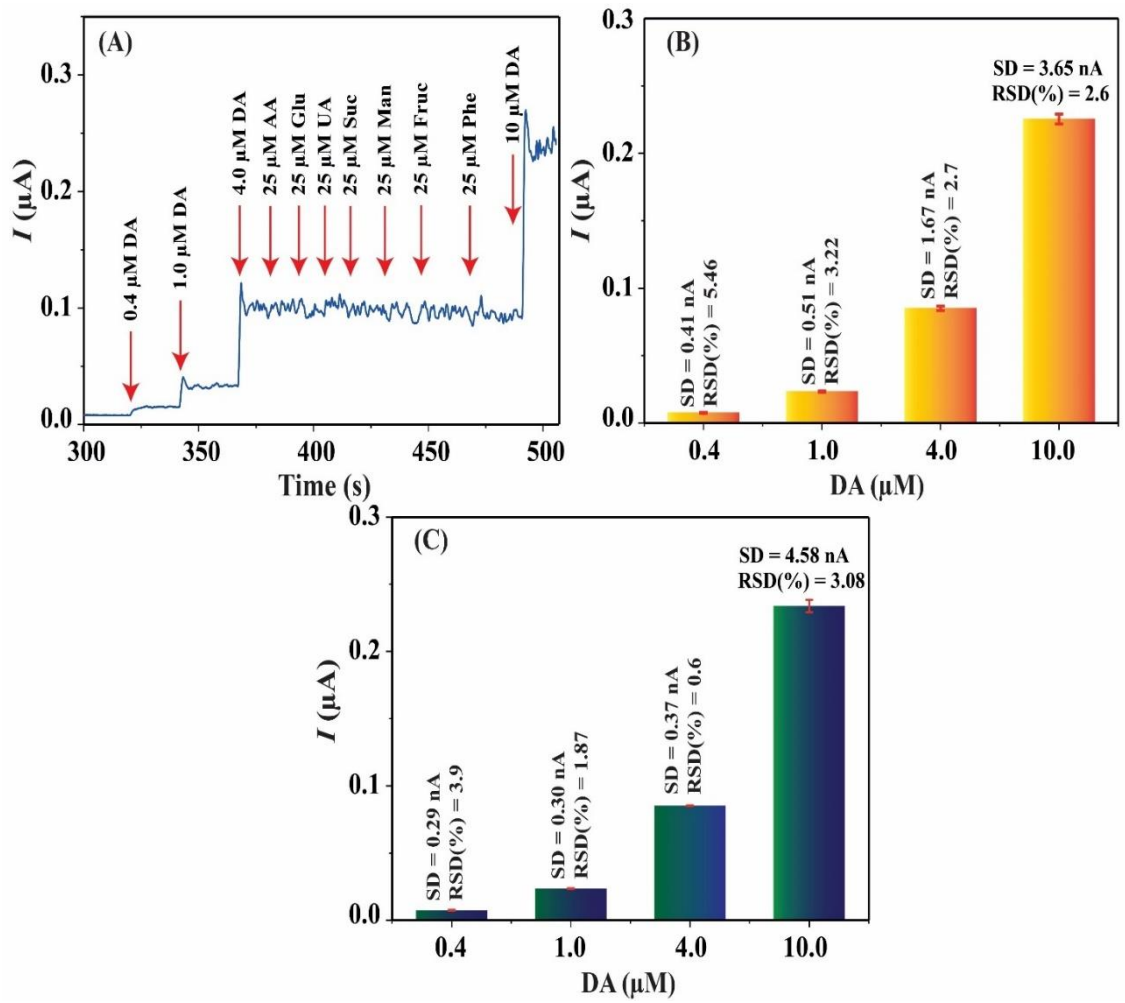

Figure 8. (A) Amperometric signals achieved at the Nf/Ni@SiO_2/GCE after adding 0.4, 1.0, 4.0 and 10.0 µM DA and 25 µM AA, UA, Phe, Glu, Fruc, Man, and Suc to BR buffer (pH 3.5). (B) The repeatability response of the sensor to DA with various amount. (C) The reproducibility of response of the sensor to DA with different concentrations.

Table 2. Electrochemical determination of dopamine in dopamine injection using Nf/Ni@SiO_2- APTES/GCE sensor

Samples	Added (µM)	Found (µM)	RSD (%)	Recovery (%)
1	0.4	0.4±0.015	3.75	100
2	1.0	1.04±0.05	4.81	104
3	4.0	4.0±0.23	5.75	100
4	10.0	10.4±0.78	7.50	104

4. Conclusion and Suggestions

In general, a novel DA electrochemical sensor was developed in this study. For this purpose, SiO_2 used as the support material was modified using APTES. Ni nanoparticles were deposited on the support. EIS, CV and amperometry were used for electrochemical studies. Ni (%5) peaks were not clearly formed in the XRD graph because Ni nanoparticles formed an amorphous structure (Ni-B) with B. The FTIR graph shows that the APTES compound was bound on the SiO_2 support. The Nf/Ni@SiO_2-APTES/GCE sensor displayed a linear detection range for DA in the range of $2x10^{-7}$ – $2.52x10^{-4}$ M. The sensitivity of the sensor was calculated to be 578.26 µA mM^{-1} cm^{-2} depending on the active surface area of the electrode using amperometric method. The LOD was computed to be 0.07 µM. The sensor exhibited extremely good

selectivity, repeatability, reproducibility and storage stability. This study showed that employing transition metal nanoparticles deposited on APTES functionalized SiO_2 is a potential method for fabricating an electrochemical sensor. Future studies may focus on new electrochemical sensors by depositing other transition metal or metal oxide nanoparticles on SiO_2-APTES.

Contributions of the authors

Yunus Emre Yıldırım: Investigation, Data curation. Muhammet Güler: Investigation, Writing, editing, Visualization, Methodology, Investigation, Data curation, Conceptualization.

Acknowledgment

This study was supported by Van Yüzüncü Yıl University, Scientific Research Projects Department (project number FYL-2021-9370).

Conflict of Interest Statement

There is no conflict of interest between the authors.

Statement of Research and Publication Ethics

The study is complied with research and publication ethics.

References

[1] S. Park, S. Park, R. A. Jeong, H. Boo, J. Park, H. C. Kim, T. D. Chung, "Nonenzymatic continuous glucose monitoring in human whole blood using electrified nanoporous Pt," *Biosens. Bioelectron.*, vol. 31, no. 1, pp. 284-291, January 2012.

[2] T. V. Maia, V. A. Conceição, "Dopaminergic disturbances in Tourette syndrome: an integrative account," *Biol. psychiatry*, vol. 84, no. 5, pp. 332-344, September 2018.

[3] O. D. Howes, R. McCutcheon, M. J. Owen, R. M. Murray, "The role of genes, stress, and dopamine in the development of schizophrenia," *Biol. psychiatry*, vol. 81, no. 1, pp. 9-20, January 2017.

[4] B. K. Madras, G. M. Miller, A. J. Fischman, "The dopamine transporter and attention-deficit/hyperactivity disorder," *Biol. psychiatry*, vol. 57, no. 11, pp. 1397-1409, October 2005.

[5] M. A. Peters, A. M. Walenkamp, I. P. Kema, C. Meijer, E. G. de Vries, S. F. Oosting, "Dopamine and serotonin regulate tumor behavior by affecting angiogenesis," *Drug Resist. Updat.*, vol. 17, no. 4-6, pp. 96-104, December 2014.

[6] J. A. Obeso, M. C. Rodríguez-Oroz, M. Rodríguez, J. Arbizu, J. M. Giménez-Amaya, "The basal ganglia and disorders of movement: pathophysiological mechanisms," *Physiol.*, vol. 17, pp. 51-55, April 2002.

[7] M. Groves, J. P. Vonsattel, P. Mazzoni, K. Marder, "Huntington's disease," *Science*, vol. 2003, pp. dn3, October 2003.

[8] M. Amiri, S. Dadfarnia, A. M. H. Shabani, S. Sadjadi, "Non-enzymatic sensing of dopamine by localized surface plasmon resonance using carbon dots-functionalized gold nanoparticles," *J. Pharm. Biomed. Anal.*, vol. 172, pp. 223-229, August 2019.

[9] X. Zhang, J. Zheng, "Hollow carbon sphere supported Ag nanoparticles for promoting electrocatalytic performance of dopamine sensing," *Sens. Actuators B: Chem.*, vol. 290, pp. 648-655, July 2019.

[10] T. W. Chen, S. Chinnapaiyan, S. M. Chen, M. A. Ali, M. S. Elshikh, A. H. Mahmoud, "A feasible sonochemical approach to synthesize $CuO@CeO_2$ nanomaterial and their enhanced non-enzymatic sensor performance towards neurotransmitter," *Ultrason. Sonochem.*, vol. 63, pp. 104903, May 2020.

[11] M. S. Wilson, "Electrochemical immunosensors for the simultaneous detection of two tumor markers," *Anal. Chem.*, vol. 77, no. 5, pp. 1496-1502, February 2005.

[12] P. D'Orazio, "Biosensors in clinical chemistry," *Clin. Chim. Acta*, Vol. 334, no. 1-2, pp. 41-69, August 2003.

[13] H. Huang, Y. Chen, Z. Chen, J. Chen, Y. Hu, J. J. Zhu, "Electrochemical sensor based on Ce-MOF/carbon nanotube composite for the simultaneous discrimination of hydroquinone and catechol," *J. Hazard. Mater.*, vol. *416*, pp. 125895, August 2021.

[14] H. V. Kiranakumar, R. Thejas, C. S. Naveen, M. I. Khan, G. D. Prasanna, S. Reddy, M. Oreijah, K. Guedri, O. T. Bafakeeh, M. Jamee, "A review on electrical and gas-sensing properties of reduced graphene oxide-metal oxide nanocomposites," *Biomass Convers. Biorefin.*, pp. 1-11, August 2022.

[15] M. Zhang, Y. Yang, W. Guo, "Electrochemical sensor for sensitive nitrite and sulfite detection in milk based on acid-treated Fe_3O_4@SiO_2 nanoparticles," *Food Chem.*, vol. 430, pp. 137004, January 2024.

[16] M. Kumar, B. K. Swamy, S. Reddy, W. Zhao, S. Chetana, V. G. Kumar, "ZnO/functionalized MWCNT and Ag/functionalized MWCNT modified carbon paste electrodes for the determination of dopamine, paracetamol and folic acid," *J. Electroanal. Chem.*, vol. 835, pp. 96-105, February 2019.

[17] L. Bayram, M. Guler, "An ultra-sensitive non-enzymatic hydrogen peroxide sensor based on SiO_2-APTES supported Au nanoparticles modified glassy carbon electrode," *Prog. Nat. Sci.: Mater. Int.*, vol. 29, no. 4, pp. 390-396, August 2019.

[18] J. Xu, J. Zhang, H. Peng, X. Xu, W. Liu, Z. Wang, N. Zhang, X. Wang, "Ag supported on meso-structured SiO_2 with different morphologies for CO oxidation: On the inherent factors influencing the activity of Ag catalysts," *Microporous Mesoporous Mater.*, vol. 242, pp. 90-98, April 2017.

[19] D. Gao, Z. Zhang, M. Wu, C. Xie, G. Guan, D. Wang, "A surface functional monomer-directing strategy for highly dense imprinting of TNT at surface of silica nanoparticles," *J. Am. Chem. Soc.*, vol. 129, no. 25, pp. 7859-7866, June 2007.

[20] M. Celebi, M. Yurderi, A. Bulut, M. Kaya, M. Zahmakiran, "Palladium nanoparticles supported on amine-functionalized SiO_2 for the catalytic hexavalent chromium reduction," *Appl. Catal. B: Environ.*, vol. 180, pp. 53-64, January 2016.

[21] I. B. Bwatanglang, S. T. Magili, I. Kaigamma, "Adsorption of phenol over bio-based silica/calcium carbonate (CS-SiO_2/$CaCO_3$) nanocomposite synthesized from waste eggshells and rice husks," *PeerJ Physical Chem.*, vol. 3, pp. e17, March 2021.

[22] C. Pereira, J. F. Silva, A. M. Pereira, J. P. Araujo, G. Blanco, J. M. Pintado, C. Freire, "[$VO(acac)_2$] hybrid catalyst: from complex immobilization onto silica nanoparticles to catalytic application in the epoxidation of geraniol," *Catal. Sci. Techno.*, vol. 1, no. 5, pp. 784-793, May 2011.

[23] Y. He, M. Qiao, H. Hu, Y. Pei, H. Li, J. Deng, K. Fan, "Preparation of amorphous Ni–B alloy: the effect of feeding order, precursor salt, pH and adding rate," *Mater. Lett.*, vol. 56, no. 6, pp. 952-957, November 2002.

[24] K. Chou, S. Chang, K. Huang, "Study on the characteristics of nanosized nickel particles using sodium borohydride to promote conversion," *Adv. Techno. Mater. Mater. Process. J.*, vol. 8, no. 2, pp. 172, January 2007.

[25] Y. Li, Y. Gu, B. Zheng, L. Luo, C. Li, X. Yan, Z. Tingting, L. Nannan, Z. Zhang, "A novel electrochemical biomimetic sensor based on poly (Cu-AMT) with reduced graphene oxide for ultrasensitive detection of dopamine," *Talanta*, vol. pp. 162, 80-89, January 2017.

[26] H. S. Jang, D. Kim, C. Lee, B. Yan, X. Qin, Y. Piao, "Nafion coated Au nanoparticle-graphene quantum dot nanocomposite modified working electrode for voltammetric determination of dopamine," *Inorg. Chem. Commun.*, vol. 105, pp. 174-181, July 2019.

[27] C. Rajkumar, B. Thirumalraj, S. M. Chen, H. A. Chen, "A simple preparation of graphite/gelatin composite for electrochemical detection of dopamine," *J. Colloid. Interface Sci.*, vol. 487, pp. 149-155, February 2017.

[28] H. Yang, D. Liu, X. Zhao, J. H. Yang, H. Chang, R. Xing, S. Liu, "AuPd bimetallic nanoparticle-supported carbon nanotubes for selective detection of dopamine in the presence of ascorbic acid," *Anal. methods*, vol. 9, no. 21, 3191-3199, May 2017.

[29] S. Hu, Q. Huang, Y. Lin, C. Wei, H. Zhang, W. Zhang, Z. Guo, X. Bao, J. Shi, A. Hao, "Reduced graphene oxide-carbon dots composite as an enhanced material for electrochemical determination of dopamine," *Electrochim. Acta*, vol. 130, pp. 805-809, June 2014.

[30] E. J. J. Laviron, "General expression of the linear potential sweep voltammogram in the case of diffusionless electrochemical systems," *J. Electroanal. Chem. Interfacial Electrochem.*, vol. 101, no. 1, pp. 19-28, July 1979.

[31] Q. J. Gong, H. X. Han, Y. D. Wang, C. Z. Yao, H. Y. Yang, J. L. Qiao, "An electrochemical sensor for dopamine detection based on the electrode of a poly-tryptophan-functionalized graphene composite," *New Carbon Mater.*, vol. *35, no.* 1, pp. 34-41, February 2020.

[32] R. Nehru, S. M. Chen, "Carbon supported olivine type phosphate framework: a promising electrocatalyst for sensitive detection of dopamine," *RSC adv.*, vol. 8, pp. 27775-27785, August 2018.

[33] A. García-Miranda Ferrari, C. W. Foster, P. J. Kelly, D. A. Brownson, C. E. Banks, "Determination of the electrochemical area of screen-printed electrochemical sensing platforms," Biosensors, vol. 8, no. 2, 53. (2018).

[34] Q. J. Gong, H. X. Han, Y. D. Wang, C. Z. Yao, H. Y. Yang, J. L. Qiao, "An electrochemical sensor for dopamine detection based on the electrode of a poly-tryptophan-functionalized graphene composite," *New Carbon Mater.*, vol. 35, pp. 34-41, February 2020.

[35] Y. Zheng, Z. Huang, C. Zhao, S. Weng, W. Zheng, X. Lin, "A gold electrode with a flower-like gold nanostructure for simultaneous determination of dopamine and ascorbic acid," *Microchim. Acta*, vol. 180, pp. 537-544, February 2013.

[36] N. S. Anuar, W. J. Basirun, M. Shalauddin, S. Akhter, "A dopamine electrochemical sensor based on a platinum–silver graphene nanocomposite modified electrode," *RSC adv.*, vol. 10, pp. 17336-17344, May 2020.

[37] Y. Y. Li, P. Kang, S. Q. Wang, Z. G. Liu, Y. X. Li, Z. Guo, "Ag nanoparticles anchored onto porous CuO nanobelts for the ultrasensitive electrochemical detection of dopamine in human serum," *Sens. Actuators B: Chem.*, vol. 327, pp. 128878, January 2021.

[38] C. Xue, Q. Han, Y. Wang, J. Wu, T. Wen, R. Wang, J. Hong, X. Zhou, H. Jiang, "Amperometric detection of dopamine in human serum by electrochemical sensor based on gold nanoparticles doped molecularly imprinted polymers," *Biosens. Bioelectron.*, vol. 49, pp. 199-203, November 2013.